



AIAA 2000–4754

**Comparison of Approximation
Models with Merit Functions for
Design Optimization**

Hyoung-Seog Chung and Juan J. Alonso
Stanford University, Stanford, CA 94305

**8th AIAA/USAF/NASA/ISSMO Symposium
on Multidisciplinary Analysis and Optimization
September 6–8, 2000/Long Beach, CA**

Comparison of Approximation Models with Merit Functions for Design Optimization

Hyoung-Seog Chung* and Juan J. Alonso†

Stanford University, Stanford, CA 94305

In this work, the use of both a second-order response surface method (RSM) and the Kriging method as approximation models for design optimization are investigated and compared. After validating the accuracy of each method with simple one- and two-dimensional analytic functions, they are applied to two Supersonic Business Jet (SBJ) drag minimization design cases in order to obtain a clear comparison of the accuracy and efficiency of these modeling techniques. A three-dimensional Euler flow solver and an automatic mesh generation capability are used in the design of a SBJ using a variety of geometric shape design parameters. The comparison results show that there is little difference in modeling accuracy and efficiency between the two methods. In addition, we find that both methods are practically applicable to realistic design optimization problems. Second-order response surface models have a severe limitation in the fact that the model of the function of interest is not a good representation for functions with multiple local minima. Although the Kriging method has the flexibility to capture multiple extrema, it exhibits limited accuracy in the estimation of global extrema. These inaccuracies depend largely on the selection of the sampling sites and the number of sample points. In the second half of this paper, merit functions are incorporated to each modeling method during the optimization process for the selection of new sample points that lead to an improvement of the current approximation model. The ability of this new procedure to identify global extrema is demonstrated using simple test functions.

Nomenclature

β	constant underlying global portion of Kriging model
β	vector of the unknown coefficients in response surface models
\mathbf{b}	vector of least squares estimators of β
C_D	drag coefficient
\mathbf{f}	constant vector used in Kriging model
L	sum of the squares of the errors
m_c	merit function
k	number of design variables
n_s	number of sample points/sites
n_t	number of test sample points to evaluate modeling error
\mathbf{r}	vector of correlation values for Kriging model
$R(\cdot)$	correlation function for Kriging model
\mathbf{R}	correlation matrix for Kriging model
RMS_{ub}	unbiased root mean square error
RS	response surface
x	scalar component of \mathbf{x}
\mathbf{x}	vector denoting all locations (sites) in the design space
\mathbf{x}^p	vector denoting the p^{th} location in the design space
\mathbf{X}	matrix of sample sites for RS model
$y(\cdot)$	unknown function

$\hat{y}(\cdot)$	estimated model of $y(\cdot)$
$\boldsymbol{\theta}$	vector of correlation parameters for Kriging model
$\hat{\sigma}^2$	estimated sample variance
ρ_c	constant controlling merit function

Introduction

THE optimization of aerospace systems is an iterative process that requires computational models embodied in complex and expensive analysis software. This paradigm is well exemplified by the field of Multidisciplinary Design Optimization (MDO) which attempts to exploit the synergism of mutually interacting disciplines in order to improve the performance of a given design, while increasing the level of confidence that the designer places on the outcome of the design itself. MDO methods greatly increase the computational burden and complexity of the design process.^{1,2} For this reason, high-fidelity analysis software typically used in single discipline designs may not be suitable for direct use in MDO.³ Faced with these problems, the alternative of using approximation models of the actual analysis software has received increased attention in recent years. A second advantage of using approximation models during the optimization process is that they can be used with optimization algorithm which do not rely on the computation of sensitivity derivatives.

One of the most common methods for building an approximate model is the response surface method

*Doctoral Candidate, AIAA Member

†Assistant Professor, Department of Aeronautics and Astronautics, AIAA Member

Copyright © 2000 by the authors. Published by the American Institute of Aeronautics and Astronautics, Inc. with permission.

(RSM) in which a polynomial function of varying order (usually a quadratic function) is fitted to a number of sample data points using least squares regression. This method has achieved popularity since it provides an explicit functional representation of the sampled data, and is both computationally inexpensive to run and easy to use. However, response surface models have several key limitations: their accuracy is only guaranteed within a small trust region, and, by design, they are unable to predict multiple extrema. In addition, these methods were originally developed to model data resulting from physical experiments which had a random error distribution. Since the nature of computer experiments is such that random errors are not present (a bias is much more common), the use of these methods for modeling deterministic data has resulted in serious debate within the statistical community.⁴ In order to overcome these problems, Sacks, et al.⁵ proposed an interpolation modeling technique, known as the Kriging method, developed in the fields of spatial statistics and geostatistics, in order to approximate the results of deterministic computer analyses. The Kriging method is different from the RSM since the interpolation of the sampled data is carried out using a maximum likelihood estimation procedure,⁶ which allows for the capturing of multiple local extrema. However, the Kriging method has higher computational cost and is harder to implement. In addition, it does not provide an explicit model function. The Kriging method also suffers from accuracy limitations which are a function of the method used for the selection of the sample points and the total number of these points.

Therefore it is important and necessary to compare these two modeling techniques and to analyze their pros and cons before using them in actual design applications. Recent studies by researchers including Simpson, et al.⁶ and Giunta, et al.⁴ have performed such comparisons in specific applications, in which they found little or no advantage in the use of Kriging methods over RSM as far as accuracy and efficiency were concerned. However, the authors strongly suggested that their conclusions were limited to the scope of their contrived applications.

In this paper, a comparison study of these two approximation methods is presented to investigate further their applicability to two design optimization test cases. A three-dimensional Euler flow solver and an automatic mesh generation capability are used in the aerodynamic design of a supersonic business jet using a variety of geometric design parameters.

The second part of this work is focused on improving the ability of the models to predict the location of global extrema. Torczon, et al.⁷ introduced the use of so-called merit functions for the selection of new sample points and for the improvement of the existing approximation model. They provided a specific

functional form that can be used within the Kriging method. The authors suggested a new merit function that is more suitable for use with RSM. Merit functions are incorporated to both approximation models during the optimization process, and their improved ability to identify a global extremum is demonstrated.

Overview of Approximation Models

Response Surface Method (RSM)

The response surface method (RSM) develops polynomial approximation models by fitting the sample data using a least squares regression technique. The true response can be written in the following form:

$$y(x) = f(x) + \epsilon, \quad (1)$$

where $f(x)$ is an unknown response function and ϵ is the random error. The response surface model of equation (1) can be written in terms of a series of observations

$$y_i = \beta_0 + \sum_{j=1}^k \beta_j x_{ij} + \epsilon_i, \quad i = 1, 2, \dots, n_s, \quad (2)$$

where n_s is the number of samples.

Equation (3) may be written in matrix form as

$$\mathbf{y} = \mathbf{X}\boldsymbol{\beta} + \boldsymbol{\epsilon}. \quad (3)$$

where

$$\mathbf{y} = \{ y_1 \quad y_2 \quad \dots \quad y_n \}^T, \quad \text{and}$$

$$\mathbf{X} = \begin{bmatrix} 1 & x_{11} & x_{12} & \dots & x_{1k} \\ 1 & x_{21} & x_{22} & \dots & x_{2k} \\ \vdots & \vdots & \vdots & & \vdots \\ \vdots & \vdots & \vdots & & \vdots \\ 1 & x_{n1} & x_{n2} & \dots & x_{nk} \end{bmatrix}.$$

$\boldsymbol{\beta}$ is a $(k+1) \times 1$ vector of the regression coefficients, and $\boldsymbol{\epsilon}$ is an $(n \times 1)$ vector of random errors.

The vector of least squares estimators, \mathbf{b} , is determined in a way that it minimizes

$$L = \sum_{i=1}^n \epsilon_i^2 = (\mathbf{y} - \mathbf{X}\boldsymbol{\beta})^T (\mathbf{y} - \mathbf{X}\boldsymbol{\beta}). \quad (4)$$

This condition simplifies to

$$\mathbf{X}^T \mathbf{X} \mathbf{b} = \mathbf{X}^T \mathbf{y}. \quad (5)$$

Thus, the least squares estimator of $\boldsymbol{\beta}$ is

$$\mathbf{b} = (\mathbf{X}^T \mathbf{X})^{-1} \mathbf{X}^T \mathbf{y}. \quad (6)$$

The reader is referred to Ref.⁸ for more details on the development of the RSM technique.

Kriging Method

The Kriging technique uses a two component model that can be expressed mathematically as

$$y(\mathbf{x}) = f(\mathbf{x}) + Z(\mathbf{x}), \quad (7)$$

where $f(\mathbf{x})$ represents a global model and $Z(\mathbf{x})$ is the realization of a stationary Gaussian random function that creates a localized deviation from the global model.⁹ $f(\mathbf{x})$ can be considered to be an underlying constant, β ,⁶ and then, equation (7) becomes

$$y(\mathbf{x}) = \beta + Z(\mathbf{x}), \quad (8)$$

which is used in this paper. The estimated model of equation (8) is given as

$$\hat{y} = \hat{\beta} + \mathbf{r}^T(\mathbf{x})\mathbf{R}^{-1}(\mathbf{y} - \mathbf{f}\hat{\beta}) \quad (9)$$

where \mathbf{y} is the column vector of response data and \mathbf{f} is a column vector of length n_s which is filled with ones. \mathbf{R} in equation (9) is the correlation matrix which can be obtained by computing $R(x^i, x^j)$, a correlation function between any two sampled data points. The correlation function is specified by the user. In this work, the authors use a Gaussian exponential correlation function of the form provided by Giunta, et al.⁴

$$R(x^i, x^j) = \exp\left[-\sum_{k=1}^n \theta_k |x_k^i - x_k^j|^2\right]. \quad (10)$$

The correlation vector between x and the sampled data points is expressed as

$$\mathbf{r}^T(\mathbf{x}) = [R(\mathbf{x}, x^1), R(\mathbf{x}, x^2), \dots, R(\mathbf{x}, x^n)]^T. \quad (11)$$

The value for $\hat{\beta}$ is estimated using the generalized least squares method as

$$\hat{\beta} = (\mathbf{f}^T \mathbf{R}^{-1} \mathbf{f})^{-1} \mathbf{f}^T \mathbf{R}^{-1} \mathbf{y}. \quad (12)$$

Since R is a function of the unknown variable θ , $\hat{\beta}$ is also a function of θ . Once θ is obtained, equation (9) is completely defined. The value of θ is obtained by maximizing the following one-dimensional functional over the interval $\theta > 0$

$$-\frac{[n \ln(\hat{\sigma}^2) + \ln |\mathbf{R}|]}{2}, \quad (13)$$

where

$$\hat{\sigma}^2 = \frac{(\mathbf{y} - \mathbf{f}\hat{\beta})^T \mathbf{R}^{-1}(\mathbf{y} - \mathbf{f}\hat{\beta})}{n_s}. \quad (14)$$

Modeling Error Estimation

Each of the approximation models were constructed based on CFD results obtained at n_s sample points. To evaluate the modeling accuracy, CFD calculations were performed at n_e randomly selected validation points and the results were compared with the predictions from the approximation models at the same

test locations. The accuracy of Kriging and RS models were compared using the unbiased root mean square (RMS) error, RMS_{ub} , the maximum error, δ_{max} , and the average % error.

The modeling error at each test site is defined as the difference between the actual result from the CFD analysis (\hat{y}_i) and the predicted value from the RS or Kriging model (y_i).

$$\delta_i = |\hat{y}_i - y_i|, \quad i = 1, \dots, n_e. \quad (15)$$

The maximum modeling error is defined as

$$\delta_{max} = \max(\delta_i), \quad (16)$$

and the average % error is defined as

$$\text{average \% error} = \frac{1}{n_e} \sum_{i=1}^{n_e} \left(\frac{\delta_i \times 100.0}{y_i} \right) \quad (17)$$

The RMS error is:

$$RMS_{ub} = \sqrt{\frac{\sum_{i=1}^{n_e} \delta_i^2}{n_e}}. \quad (18)$$

Supersonic Business Jet Design Test Problems

This design problem involves the drag minimization of a supersonic business jet wing-body configuration at a specified lift coefficient. The aircraft geometry and flow conditions were parameterized with a total of 22 potential design variables of which a subset is used in the following two test cases.

Case I : 7 Design Variable Case

For the initial test case, total of 7 geometric design variables were used. The chosen design variables represent the radii at three different stations along the axisymmetric fuselage, ($x_1 \rightarrow x_3$), and the thickness to chord ratios at four span-wise stations ($x_4 \rightarrow x_7$). The airfoil shape for all wing stations was selected as a simple biconvex airfoil of varying thickness. Once the design variables were selected, an automatic mesh generation procedure that was able to handle the geometry variations imposed by the changes in the design variables was utilized to automatically generate different sets of meshes needed for the CFD calculations.

The three-dimensional Euler solver, FLO87, developed by Jameson^{10,11} was used to calculate aerodynamic coefficients at sample design points chosen by incrementing each variable from the baseline design value using a Design of Experiments approach. The free-stream flow conditions were fixed at $M_\infty = 2.0$ and the coefficient of lift, based on the wing planform area was fixed at $C_L = 0.1$. Response surface and Kriging models were built using drag output data from the Euler solver, and were incorporated into a non-linear constrained optimization code named SNOPT which has been developed by Gill, et al.¹² to perform realistic design optimization calculations.

Case II : 14 Design Variable Case

The design test problem was extended to a total of 14 design variables to further investigate and compare the model accuracy and applicability in higher dimensionality design spaces. Figure 1 shows the definition of the design variables, which include wing sweep angle (x_1), wing aspect ratio (x_2), wing taper ratio (x_3), leading and trailing edge extensions as ratios of wing root chord (x_4, x_5), thickness-to-chord ratios at three span-wise stations ($x_6 \rightarrow x_8$), wing twist angles at three span-wise stations ($x_9 \rightarrow x_{11}$), and radii at three different stations along the axisymmetric fuselage ($x_{12} \rightarrow x_{14}$). The sequence of mesh generation, CFD analysis, approximation construction and constrained optimization process remained the same as for Case I.

Design Tools

Grid Generator

A grid generator called CH-GRID developed by Reuther et al. was used for mesh generation of supersonic business jet wing-body configurations. CH-GRID is a stand-alone form of the C-H type grid generator that we use for our single-block wing-body design code. Figure 2 shows an example of a typical wing-body mesh.

Flow Solver

The CFD flow solver must meet fundamental requirements of accuracy, efficiency, robustness, and fast convergence to be used in a high-dimensional design optimization problem. The accuracy is important because the approximation model accuracy and the improvement predicted by the optimization process using the models can only be as good as the accuracy of the flow analysis. Efficiency is also required when the number of design variables increases and the required number of the sample evaluations for constructing the approximation models increases accordingly. The robustness of the solver, i.e., its ability to obtain a flow solution for a variety of configuration shapes and flow conditions, is particularly critical for the construction of sample database for the approximation models, in which a large variation of the values of the design variables is allowed. In addition, the benefit of aerodynamic optimization lies in obtaining the last few percentage points in aerodynamic efficiency. In such cases, the solution must be highly converged such that the noise in the figure of merit is well below the level of realizable improvement.¹³

Jameson's FLO87 code used in this study easily met all of the previously mentioned criteria. FLO87 solves the steady three-dimensional Euler equation using a modified explicit multistage Runge-Kutta time stepping scheme. FLO87 achieves fast convergence with the aid of multigriding and implicit residual smoothing. Also, a driver program called RS87 was developed

to utilize multiprocessor computers for analyzing a number of different configurations at the same time.

Optimization Routine

Optimization of wing-body configurations was performed using an optimization program called SNOPT. SNOPT uses a sequential quadratic programming (SQP) algorithm that obtains search directions from a sequence of quadratic programming subproblems.¹² Nonlinear constraints were imposed on the minimization process by setting bounds for the values of the design variables, and constraining the admissible ranges of wing (wv) and fuselage volumes (fv). The optimization problem can be written as

$$\min_{x \in R^m} C_D(x), \quad (19)$$

subject to

$$\begin{aligned} 0.8 \times wv_i &\leq wv \leq 1.2 \times wv_i \\ 0.8 \times fv_i &\leq fv \leq 1.2 \times fv_i \\ x_{min} &\leq x \leq x_{max} \end{aligned}$$

where wv_i and fv_i are the initial wing and fuselage volumes.

Approximation Models with Merit Functions

The accuracy of predicting a global extremum with the presented approximation models is limited by the quadratic nature of the RSM and by the number of sample points and their locations for the Kriging model. Torczon, et al.⁷ introduced the use of so-called merit functions for selecting new sample points and for improving the global approximation ability of the model as the optimization algorithm proceeds. They also demonstrated the applicability of their suggestion to the Kriging model with a simple one-dimensional example. In this work, we expand the application of this technique to a two-dimensional example used for the graphical validation. The merit function suggested by Torczon, et al is used

$$m_c(\mathbf{x}) = a_c(\mathbf{x}) - \rho_c d_c(\mathbf{x}), \quad (20)$$

where a_c represents an approximation model and ρ_c is a positive real number which is dependent on the specific application. $d_c(\mathbf{x})$ is the distance from \mathbf{x} to the nearest previous sample point.

$$d_c(\mathbf{x}) = \min \|\mathbf{x} - \mathbf{x}_i\|_2 \quad (21)$$

Once $m_c(\mathbf{x})$ is found, the new sampling site is selected by finding the location of the minimum of m_c . Therefore, m_c is only used for computing the location of the new sample point.

The authors have found that a slight modification of the form of merit function given by Torczon, et al. is

more suitable for the RSM, and suggest the following form

$$m_c(\mathbf{x}) = a_c(\mathbf{x}) - (\rho_c d_c(\mathbf{x}))^2. \quad (22)$$

The value of ρ_c was obtained by trial and error. In this case, $\rho_c = 500$ worked well. The selection of the optimal value for ρ_c is a subject of further study.

Results and Discussion

Graphical Validation of RSM and Kriging

For graphical validation of RS and Kriging methods, an analytic test function called the *peaks* function was chosen from the MATLAB User's Guide¹⁴ as shown in Figure 3(a). Sample data were obtained at six different locations, from which RS and Kriging models were constructed. The sample data points for the Kriging model were selected to be scattered around the peaks while those for the RS model were selected to be concentrated around the global minimum point. Figure 3(b) shows the shape of Kriging model that has all the general features of the test function. The RS models are shown as the shaded surface in Figures 3(c) and (d). These graphical examples clearly indicate the ability of both methods to model the original function.

To further investigate their feasibility to model the original CFD code, 7-dimensional RS and Kriging models were created for test Case I from the C_D data obtained from CFD analyses at 36 different design sites within the design space. One and two-dimensional slices of the 7-dimensional approximation models are plotted in Figure 4 for the first and fifth design variables, corresponding to the radius of a fuselage station ahead of the leading edge of the wing, and to the t/c ratio of the wing station located right at the side-of-body. Additional runs of the flow solver are included to get a feeling for the accuracy of the presented techniques. The RS and Kriging methods appear to resolve the function of interest (coefficient of drag) quite well over a wide range of values of the design variables.

Design of Experiments for RS

In general, the second-order RS model has the form

$$\hat{y} = \beta_0 + \sum_{j=1}^k \beta_j x_j + \sum_{i < j} \beta_{ij} x_i x_j, \quad (23)$$

in which there are $(k+1)(k+2)/2$ coefficients to be estimated, where k is the number of variables. When constructing a quadratic model, the design variables need to be evaluated at least at 3 levels to estimate the coefficients in the model. This leads to 3^k factorial design of experiments that requires 3^k number of sample data evaluations. However, the Central Composite Design (CCD) technique introduced by Box, et al.¹⁵ became a popular alternative design for the second-order RS model. The CCD technique is a first-order (2^k) design augmented by additional points to allow estimation of the second-order coefficients.¹⁶

Unal, et al.³ found out that CCD enabled the efficient construction of a second-order RS models with significantly less effort than a full factorial design, and the fitted model could be successfully used in MDO process with reasonable accuracy for cases with four to six design variables. However, for design problems dealing with a large number of design variables, even CCD becomes unrealistic in the optimization process.

In this work, two designs of experiment methods were investigated for test Case I. The first one was CCD and the second one was the minimum point design (MPD). The number of function evaluations needed for MPD is exactly equal to the number of coefficients in the RS model. Thus, the minimum number of CFD calculations needed to construct a RS model for 7-dimensional design problem is 36, while that for CCD is 143 with only one center point. Table 1 shows a comparison of the two design methods. First, RS models were constructed based on data collected from MPD and CCD, and their accuracy was tested over another set of 72 test sample points. The results show that the RS model using MPD has lower RMS and average % error than that using CCD although the differences are small. One optimization cycle was carried out and results also showed almost same trends in predicted optimum value of C_D and design variables. One interesting point is that the results from the first optimization cycle using the CCD based RS model are really close to those from the 3rd optimization cycle using the minimum point design as shown in Table 3. Therefore, the authors reached the conclusion that the CCD-based RS model generally has a better ability to locate the minimum point in fewer design iteration; however, the sequential optimization process using the RS model with MPD has almost same ability with less computational cost since the required CFD evaluations for three optimization cycles with MPD is 108 whereas one CCD iteration requires 143 flow solutions. Based on the comparison, it was decided to use MPD for the rest of the work presented in this paper. The number of CFD evaluations required for an MPD of test Case II is 120.

Determination of Correlation Parameters for Kriging Model

It is found that the accuracy of Kriging models largely depends on the values of the correlation parameters defined in Equation 10. However, the determination of θ requires another optimization process for equation 13, which imposes extra difficulties. To illustrate this problem, an one-dimensional analytic function was tested for four different cases as shown in Figure 5.

For the first case, three sample data points were chosen and the Kriging model was constructed as shown in Figure 5(a). The accuracy of the model is generally poor except a certain interval. In Figure 5(b), the

functional value of equation 13 is plotted against θ . It shows that the value of equation 13 keeps increasing and the selected value of θ based on maximizing equation 13 becomes too large, which, in turn, degrades the accuracy of the model. Three different ways to correct the problem are suggested in the following figures. The first method is to increase the number of sample data points. Inaccuracies in Figure 5(a) are clearly due to under-sampling. If the number of sample data points is increased to five, the accuracy of the model in the region of the local minimum is greatly improved. Note that the plot of Equation 13 vs. θ for this case has a clear maximum in the lower range of values of θ . The second method is to limit the maximum value of θ while still using three sample points. The resulting model is presented in Figure 5(e), and it can be seen that the model accuracy has improved considerably. The last method is to use gradient information. Figure 5(g) shows the simulation of using gradient information by sampling the points very close to the original sites. The results also show that the accuracy has been greatly improved, and the shape of the plot of Equation 13 vs. θ is changed to one that has a distinct maximum, which reduces the difficulty of selecting the value of θ . The last method leads to the need for further work on utilizing gradient information to improve the accuracy and efficiency of approximation models. The tests presented above identify that successful Kriging model construction is dependent on the selection of the number of sample points and their locations as well as the corresponding values of the correlation parameters. Also note that, even though the Kriging model is supposed to have the ability of global modeling, this advantage can be seriously impaired by the choice of the number of sample points and their locations.

The authors had difficulties determining the right values of the correlation parameters for the 14 variable supersonic business jet design problem. The maximization procedure for Equation 13 resulted in the unbounded problem. The problem, which seemed to be caused by under-sampling, was solved by manually searching for optimum values of the parameters and checking the error metrics over a set of test sample data.

Modeling Accuracy Comparison

Once the approximation models were created, their modeling accuracy was compared using four error metrics. The results of the comparison is summarized in Table 2. The error metrics were estimated over 72 test sample points for Case I and over 120 test sample points for case II. The results for the Case I test problem indicate that the accuracy of both models is about the same. But, for Case II, the RS model turned out to have better accuracy than the Kriging model. It is observed that the results are mainly due to the diffi-

culties in selecting the optimal correlation parameters for Kriging model as mentioned earlier in Section .

Optimization Efficiency Comparison

A. Case I : 7 Variable Supersonic Business Jet Design

The baseline design point for Case I was $x_1=0.45$, $x_2=0.45$, $x_3=0.3$, x_4 $x_7=2.0(\%)$. The design variables are defined in Section . The design optimization process was performed using RS and Kriging models with the following limits on design variables and constraints:

$$0.8 \times wv_i \leq wv \leq 1.2 \times wv_i$$

$$0.8 \times fv_i \leq fv \leq 1.2 \times fv_i$$

$$0.35 \leq x_1 \leq 0.55$$

$$0.35 \leq x_2 \leq 0.55$$

$$0.20 \leq x_3 \leq 0.40$$

$$1.60 \leq x_4 \leq 2.40$$

$$1.60 \leq x_5 \leq 2.40$$

$$1.60 \leq x_6 \leq 2.40$$

$$1.60 \leq x_7 \leq 2.40$$

where wv_i and fv_i are the initial wing and fuselage volumes. The complete results from three design iterations are listed in Table 3.

As shown in Table 3, the predicted optimum design point and optimum value of C_D for both the RS and Kriging models are nearly identical. After the third cycle, the predicted C_D with the RS model is 0.0072704 whereas that for the Kriging model is 0.0072702 with almost same optimum location. Note that the fuselage radii defined just forward of wing (x_1) and aft of wing (x_2) tend to increase slightly during the optimization process in agreement with results from the supersonic area rule. Also, the thickness-to-chord ratios, except the one defined at a wing station inside of the fuselage(x_4), all tend to decrease to the imposed limit of 1.6% in order to minimize the supersonic drag due to volume. A total reduction of 5.5 % in C_D was achieved for both cases.

A. Case II : 14 Variable Supersonic Business Jet Design

To further investigate the applicability of both approximation methods in more realistic design problem, Case I was extended to a total of 14 design variables. The definitions of the 14 design variables used in the Case II are shown in Figure 1. The baseline design points and the limits imposed on each variable are listed below:

$$0.0719 \leq x_1(base = 4.0719) \leq 8.0719$$

$$2.4995 \leq x_2(base = 2.6995) \leq 2.8995$$

$$\begin{aligned}
0.3001 &\leq x_3(\text{base} = 0.3501) \leq 0.4001 \\
0.00 &\leq x_4(\text{base} = 0.00) \leq 0.30 \\
0.00 &\leq x_5(\text{base} = 0.00) \leq 0.20 \\
1.60 &\leq x_6(\text{base} = 2.00) \leq 2.40 \\
1.60 &\leq x_7(\text{base} = 2.00) \leq 2.40 \\
1.60 &\leq x_8(\text{base} = 2.00) \leq 2.40 \\
-2.00 &\leq x_9(\text{base} = 0.00) \leq 2.00 \\
-2.00 &\leq x_{10}(\text{base} = 0.00) \leq 2.00 \\
-2.00 &\leq x_{11}(\text{base} = 0.00) \leq 2.00 \\
0.35 &\leq x_{12}(\text{base} = 0.45) \leq 0.55 \\
0.35 &\leq x_{13}(\text{base} = 0.45) \leq 0.55 \\
0.20 &\leq x_{14}(\text{base} = 0.30) \leq 0.40
\end{aligned}$$

The results of two design iterations are also summarized in Table 3. As in Case I, both approximations predicted generally the same design with minor differences in some of the design variables. The optimum design point found in the second cycle for the optimization using the Kriging model was worse than that obtained from the first design cycle. Again, it is inferred that this drawback resulted from the difficulty in determining the correlation parameters, θ .

The optimization process managed to reduce C_D by 12.4 % with the RS model and by 12.3 % with the Kriging model over the baseline configuration. Even though it took more computational time for the optimization with the Kriging model, the difference is practically negligible considering the time required for the CFD function evaluations: the difference in execution time was of the order of a couple of minutes. Overall, the two approximation methods were found to be applicable to all of the test problems presented in this paper.

Global Optimization Using Merit Functions

One major advantage of the Kriging model is that it can model functions with multiple extrema and can be used in a global optimization process, in contrast with an RS model which only can model local extrema. However, as shown in Figure 5, the ability of a Kriging model to locate the global minimum can be greatly diminished depending on the locations and the number of the sample points. The weaknesses of the approximation models investigated in this study can be greatly improved by using a so-called merit function as suggested by Torczon et al.⁷

A one-dimensional example of the optimization using an RS model with a merit function is also suggested by authors and is presented in Figure 6. The merit function is constructed in such a way that it has a global minimum at the point where the least amount of information on the function is known. The next sample point in the search for a global minimum is selected by the merit function and not by the actual model prediction of the location of the minimum. Since there

are three coefficients in a one-dimensional quadratic RS model, only three sample points are used in the sequential optimization process. The original three sample points are located around the local minimum at $x = 0.35$. The merit function is formed with the RS model and the data on the current three sample points. In the first iteration, the merit function has a global minimum at $x = 0.0$. Then, the algorithm samples the functional value at that point and compares it with the current minimum value. If the new value is lower than the current minimum, it replaces the current minimum site and two new sample points closer to the updated minimum location are selected. Otherwise this new point is disregarded. Since, in the example, the functional value at $x = 0.0$ is greater than the current minimum at $x = 0.35$, the former is disregarded and the sample data and RS model remain the same as shown in Figure 6(b). However, in the second iteration, the merit function predicts a global minimum at $x = 0.14$. The functional value at that point is less than the current minimum point and therefore, for the next iteration, a new set of three sample data points which are in the neighborhood of $x = 0.14$ are selected and the RS model is updated with the new sample data. The procedure is continued until the difference between the minimum values from the RS model and the merit function becomes small. Figure 6(h) shows the result after 10 iterations of the procedure. The RS model now has the improved ability to be able to locate the global minimum with the aid of the merit function as demonstrated in Figure 6.

A two-dimensional demonstration of the procedure using the RS model is shown in Figure 8. The figures show that the initial tendency to converge to a local minimum is changed and that the model correctly finds the global minimum point.

A two-dimensional demonstration of the Kriging method global optimization capability using a merit function is also presented in Figure 7. Each subsequent model is updated with a new added sample point which is located at the global minimum obtained using the merit function at previous step.

One major problem in this procedure is to determine the value of ρ_c to be used in Equations 20 and 22. If ρ_c is too large, the convergence to the global minimum will take a long time, but, if it is too small, the models can not escape from the local minimum point close to the starting design. The right choice of ρ_c value is the key to the successful and practical application of this method to a realistic optimization problem, and it is the subject of current and future work.

Conclusions

In this study, the accuracy of RS and Kriging methods and their applicability in a realistic design optimization problem have been evaluated and compared. The results from the two test cases indicate that both

methods have comparable modeling accuracy and ability to locate an optimum design point. However, it is pointed out that the Kriging procedure requires one more optimization step for determining the correlation parameters which might cause some difficulties in high-dimensional design problems. The computational time to construct and to use the Kriging model in the design process is higher than that required for RS models, but the difference was negligible at least for the test cases investigated in this work.

The ability of the approximation models to locate a global minimum can be greatly improved by the use of a merit function. In the paper, we have shown that even the RS model can be used in a global optimization process. This has been shown for both one- and two-dimensional problems of pre-conceived topology. Future work will address the applicability of the merit function approach to multi-dimensional problems in supersonic business jet design.

Future Work

The present study has identified several areas that require further investigation. These areas include: (1) research on a robust method to determine the correlation parameter that can be used as an alternative to the time consuming method of maximizing Equation 13, (2) the utilization of gradient information from adjoint methods for improving the accuracy and efficiency of the approximation model construction, (3) the selection of a criteria for the calculation of the value of ρ_c in Equations 20 and 22, and (4) the testing of merit functions in more realistic design application.

References

- ¹Thomas A. Zang and Lawrence L. Green. "Multidisciplinary Design Optimization Techniques: Implications and Opportunities for Fluid Dynamics," *30th AIAA Fluid Dynamics Conference*, Norfolk, Virginia, AIAA 99-3798, June 1999
- ²Jaroslav Sobieszczanski-Sobieski and Raphael T. Haftka "Multidisciplinary Aerospace Design Optimization: Survey of Recent Developments," *34th AIAA Aerospace Sciences Meeting and Exhibit*, Reno, Nevada, AIAA 96-0711, January 1996.
- ³Resit Unal, Roger A. Lepsch, Jr. and Mark L. McMillin "Response Surface Model Building and Multidisciplinary Optimization Using Overdetermined D-Optimal Designs," *7th AIAA/USAF/NASA/ISSMO Symposium on Multidisciplinary Analysis and Optimization*, St. Louis, Missouri, AIAA 98-4759, September 1998
- ⁴Anthony A. Giunta and Layne T. Watson "A Comparison of Approximation Modeling Techniques: Polynomial Versus Interpolating Models," *7th AIAA/USAF/NASA/ISSMO Symposium on Multidisciplinary Analysis and Optimization*, St. Louis, Missouri, AIAA 98-4758, September 1998.
- ⁵J. Sacks, W. J. Welch, T. J. Michell, and H. P. Wynn "Design and Analysis of Computer Experiments," *Statistical Science Vol 4, No.4*, pp. 409-453, 1989
- ⁶Timothy W. Simpson, Timothy M. Mauery, John J. Korte and Farrokh Mistree "Comparison of Response Surface and Kriging Models in the Multidisciplinary Design of an Aerospike Nozzle," *7th AIAA/USAF/NASA/ISSMO Symposium on Multidisciplinary Analysis and Optimization*, St. Louis, Missouri, AIAA 98-4755, September 1998

- ⁷Virginia Torczon and Michael W. Trosset "Using Approximation to Accelerate Engineering Design Optimization," *ICASE Report 98-33*, Hampton, Virginia, 1998
- ⁸Raymond H. Myers and Douglas C. Montgomery *Response Surface Methodology: Process and Product Optimization Using Designed Experiments*, John Wiley, New York, 1995.
- ⁹J. R. Koehler and A. B. Owen "Computer Experiments," *Handbook of Statistics Vol. 13*, pp. 261-308, Elsevier Science, New York, eds. S. Ghosh and C. R. Rao
- ¹⁰A. Jameson, W. Schmidt, and E. Turkel "Numerical Solutions of the Euler Equations by Finite Volume Methods with Runge-Kutta Time Stepping Schemes," *AIAA Paper 81-1259*, Jan. 1981.
- ¹¹A. Jameson "Multigrid Algorithms for Compressible Flow Calculations," *Lecture Note in Mathematics* edited by W. Hackbusch and V. Trottenberg, Vol. 1228, Springer-Verlag, 1986.
- ¹²Philip E. Gill, Walter Murray and Michael A. Saunders "User's Guide for SNOPT 5.3: A Fortran Package for Large-scale Nonlinear Programming," *Technical Report SOL 98-1* Dept. of Engineering Economic Systems and Operations Research, Stanford Univ., Stanford, CA, 1998
- ¹³James J. Reuther, Antony Jameson, and Juan J. Alonso "Constrained Multipoint Aerodynamic Shape Optimization Using an Adjoint Formulation and Parallel Computers, Part I," *Journal of Aircraft* Vol 36, No 1, January-February, 1999
- ¹⁴*MATLAB User's Guide for Unix Workstations*, The MathWorks, Inc. Mass., August 1992, January-February, 1999
- ¹⁵G. E. Box, and K. B. Wilson, "On the experimental Attainment of Optimum Conditions," *Journal of the Royal Statistical Society Series B*, 13, 1-45.
- ¹⁶G. E. Box, and N. R. Draper, *Empirical Model Building and Response Surfaces*, John Wiley, New York, NY, 1987.

Design of Experiment	Model Accuracy Comparison		Optimization Comparison			
	RMS	Ave. % Error	1 st Design Cycle Results	Predicted Optimum (C _D)	Verified Optimum by CFD	% Error
Minimum Point Design	1.098E-4	0.7256 %	x ₁ =0.482 x ₂ =0.418 x ₃ =0.286 x ₄ =1.653 x ₅ ~x ₇ =1.600	0.007287	0.007305	0.244 %
Central Composite Design	1.867E-4	0.9856 %	x ₁ =0.481 x ₂ =0.441 x ₃ =0.325 x ₄ =2.400 x ₅ ~x ₇ =1.600	0.007276	0.007271	0.069 %

Table 1. Comparison of Design of Experiments for RS over 72 test sample points for Case I.

Model	Case I : 7 Variable SBJ Design (72 test samples)				Case II : 14 Variable SBJ Design (120 test samples)			
	RMS _{ub}	Ave. % Error	Mean Error	Max Error	RMS _{ub}	Ave. % Error	Mean Error	Max Error
RSM	0.000110	0.726 %	0.0000648	4.03 %	0.00000234	0.197 %	0.0000142	0.959 %
Kriging	0.000118	0.855 %	0.0000748	4.13 %	0.00004597	0.568 %	0.0000408	1.425 %

Table 2. Modeling Accuracy Comparison

		Case I : 7 Variable SBJ Design			Case II : 14 Variable SBJ Design	
		1 st Design Cycle	2 nd Design Cycle	3 rd Design Cycle	1 st Design Cycle	2 nd Design Cycle
RS Model	Optimum Design	x ₁ =0.4816 x ₂ =0.4177 x ₃ =0.2862 x ₄ =1.653 x ₅ =1.600 x ₆ =1.600 x ₇ =1.600	x ₁ =0.4770 x ₂ =0.4460 x ₃ =0.3313 x ₄ =2.400 x ₅ =1.600 x ₆ =1.600 x ₇ =1.600	x ₁ = 0.4811 x ₂ = 0.4425 x ₃ = 0.3247 x ₄ = 2.400 x ₅ = 1.600 x ₆ = 1.600 x ₇ = 1.600	x ₁ =3.8675, x ₂ =2.7449 x ₃ =0.3564, x ₄ =0.2583 x ₅ =0.1999, x ₆ =1.600 x ₇ =1.600, x ₈ =1.970 x ₉ =-0.122, x ₁₀ =-0.329 x ₁₁ =0.098, x ₁₂ =0.4825 x ₁₃ =0.4179, x ₁₄ =0.3041	x ₁ =3.5446, x ₂ =2.8995 x ₃ =0.3528, x ₄ =0.300 x ₅ =0.200, x ₆ =1.600 x ₇ =1.600, x ₈ =1.807 x ₉ =-0.381, x ₁₀ =-1.273 x ₁₁ =0.427, x ₁₂ =0.4883 x ₁₃ =0.4351, x ₁₄ =0.3125
	Predicted Optimum	0.0072871	0.0072762	0.0072661	0.0068465	0.0067551
	Verified Optimum*	0.0073049	0.0072714	0.0072704	0.0068977	0.0067374
	% Error	0.244 %	0.066 %	0.059 %	0.748 %	0.262 %
Kriging Model	Optimum Design	x ₁ =0.4805 x ₂ =0.4278 x ₃ =0.3046 x ₄ =1.7863 x ₅ =1.600 x ₆ =1.600 x ₇ =1.600	x ₁ =0.4789 x ₂ =0.4440 x ₃ =0.3262 x ₄ =2.400 x ₅ =1.600 x ₆ =1.600 x ₇ =1.600	x ₁ = 0.4812 x ₂ = 0.4441 x ₃ = 0.3263 x ₄ = 2.400 x ₅ = 1.600 x ₆ = 1.600 x ₇ = 1.600	x ₁ =5.4505, x ₂ =2.8995 x ₃ =0.3221, x ₄ =0.300 x ₅ =0.200, x ₆ =1.600 x ₇ =1.600, x ₈ =1.600 x ₉ =0.368, x ₁₀ =-0.338 x ₁₁ =0.815, x ₁₂ =0.4870 x ₁₃ =0.4347, x ₁₄ =0.3351	x ₁ =5.7175, x ₂ =2.8995 x ₃ =0.3221, x ₄ =0.300 x ₅ =0.200, x ₆ =1.600 x ₇ =1.600, x ₈ =1.600 x ₉ =0.783, x ₁₀ =0.118 x ₁₁ =1.364, x ₁₂ =0.4827 x ₁₃ =0.4313, x ₁₄ =0.3194
	Predicted Optimum	0.0072883	0.0072766	0.0072669	0.0066468	0.0066859
	Verified Optimum*	0.0072879	0.0072707	0.0072702	0.0067303	0.0067464
	% Error	0.005 %	0.081 %	0.046 %	1.240 %	0.896 %

Table 3. Optimization Results using RS and Kriging Models
(* Calculated using CFD analysis code with predicted optimum design)

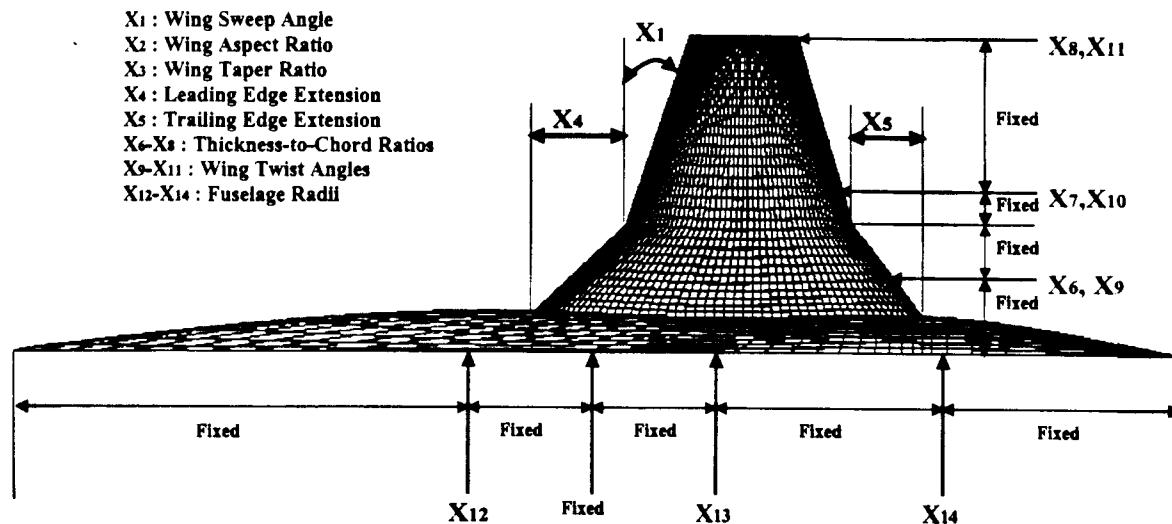


Fig. 1 Definition of Design Variables for SBJ Wing-Body Configuration

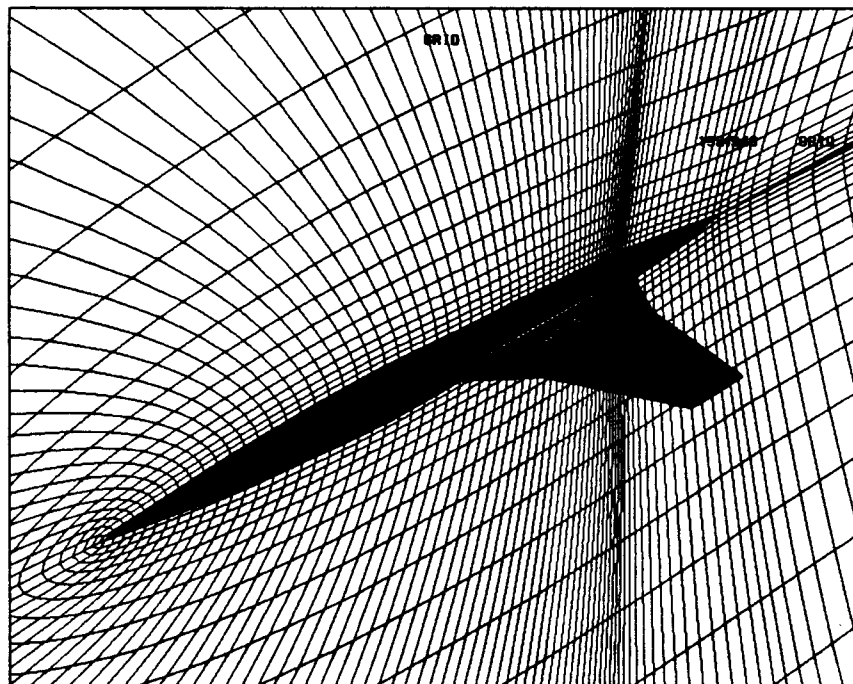
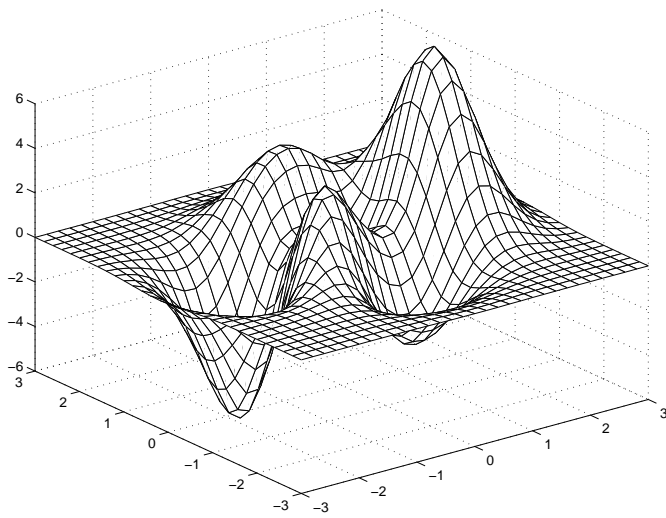
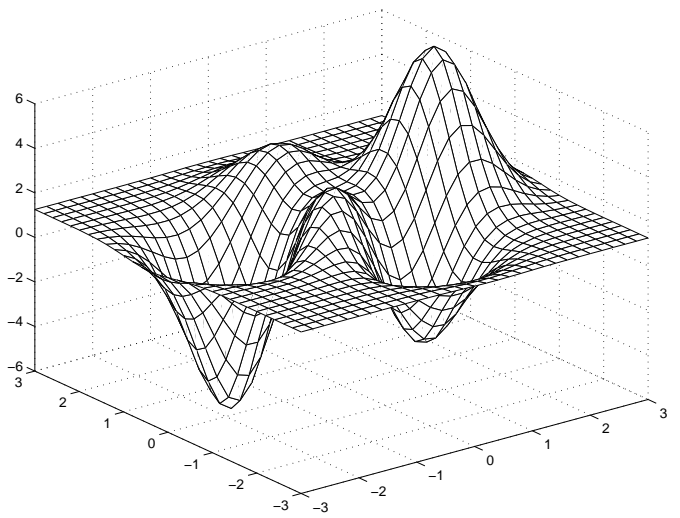


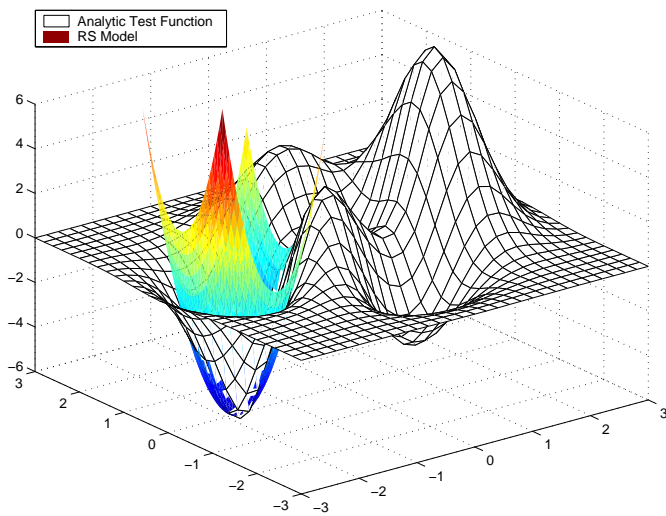
Fig. 2 A Typical Supersonic Business Jet Mesh for CFD Calculation



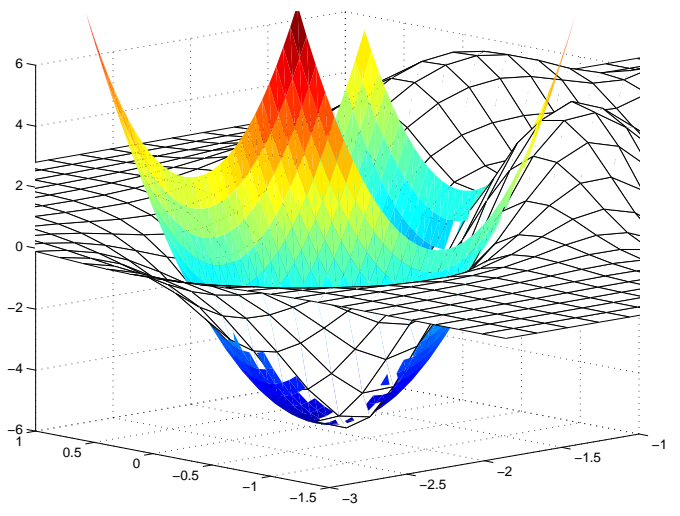
(a) 2-D Analytic Test Function



(b) Kriging Model (6 sample points)

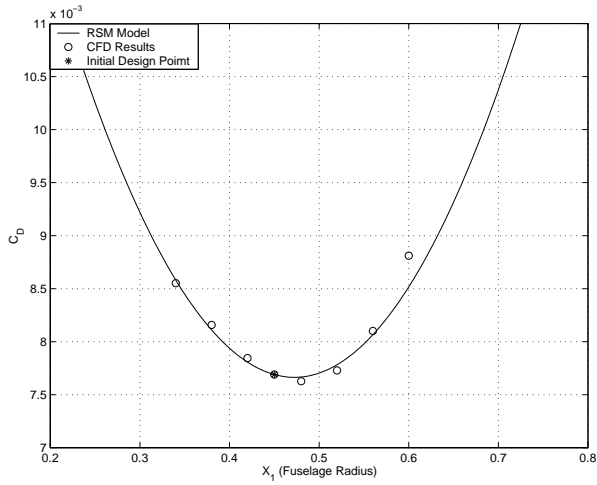


(c) RS Model (6 sample points)

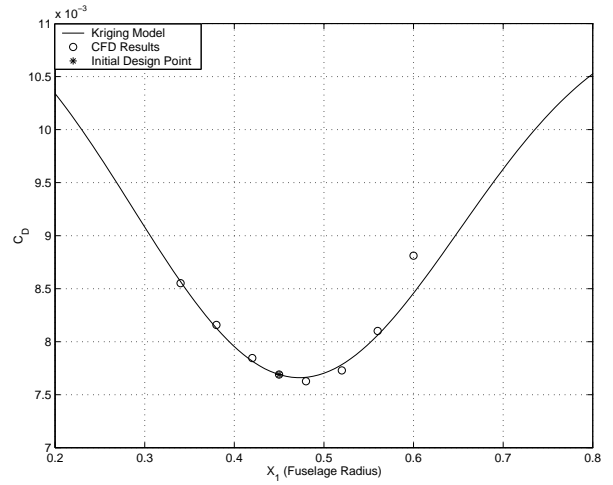


(d) RS Model (enlarged)

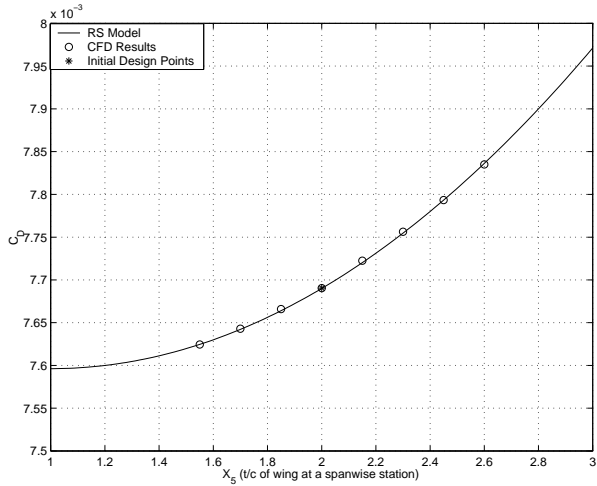
Fig. 3 Graphical Validation of Approximation Models with 2-D Test Function



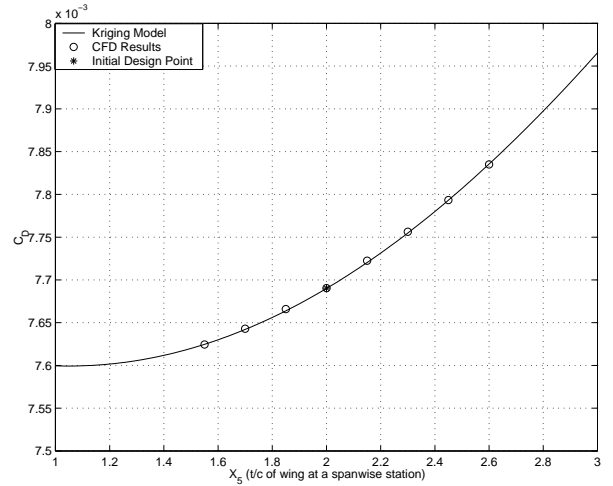
(a) RS Model 1-D Slice Check for X_1 (all other design variables fixed)



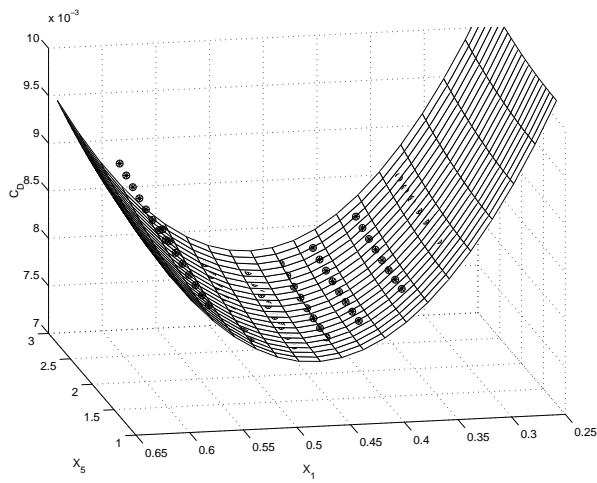
(b) Kriging Model 1-D Slice Check for X_1 (all other design variables fixed)



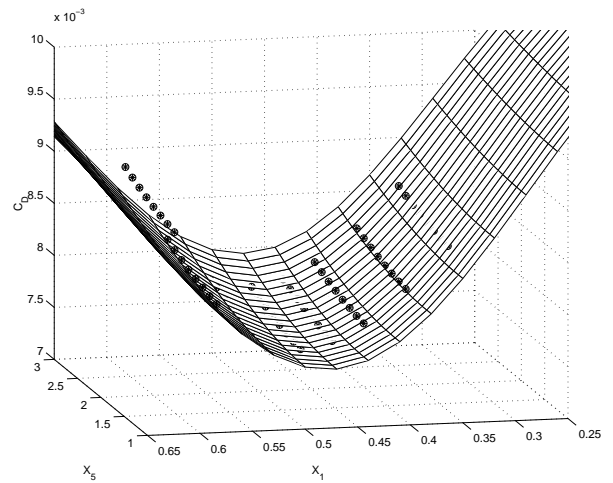
(c) RS Model 1-D Slice Check for X_3 (all other design variables fixed)



(d) Kriging Model 1-D Slice Check for X_3 (all other design variables fixed)

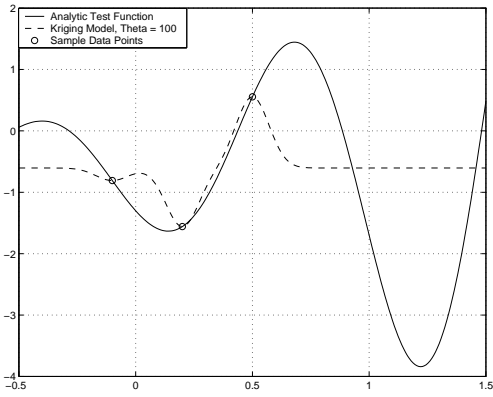


(e) RS Model 2-D Slice Check for X_1 - X_3 (all other design variables fixed)

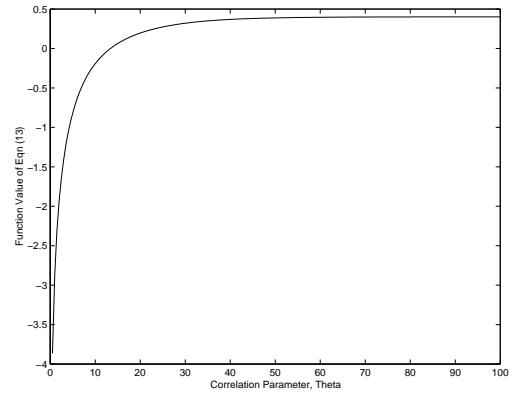


(f) Kriging Model 2-D Slice Check for X_1 - X_3 (all other design variables fixed)

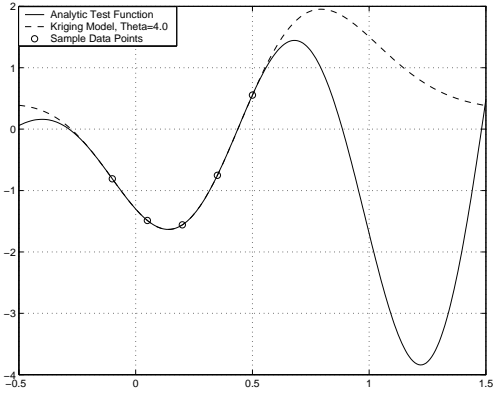
Fig. 4 Graphical Validation of Approximation Models for Test Case I



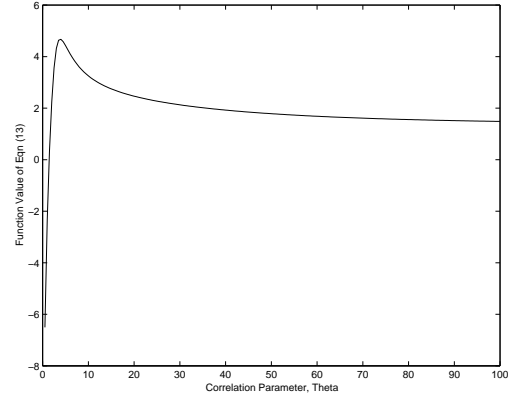
(a) 1-D Kriging Model with 3 Sample Points



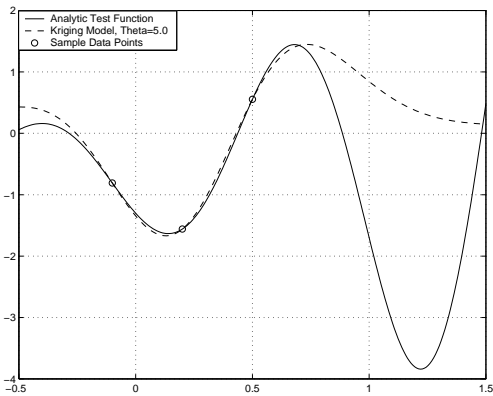
(b) Eqn(13) vs. θ for case a.



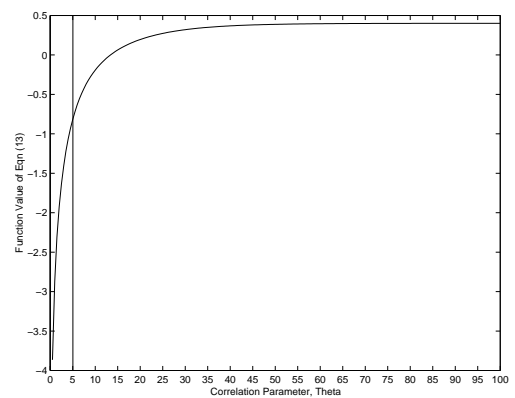
(c) 1-D Kriging Model with 5 Sample Points



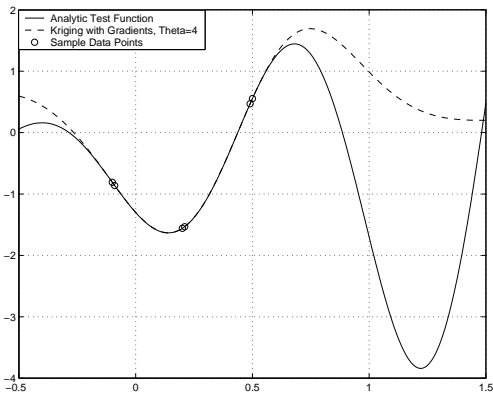
(d) Eqn(13) vs. θ for case c.



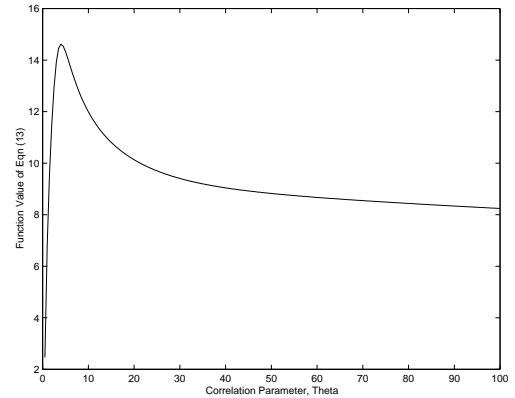
(e) Kriging Model with 3 Sample Points ($\theta = 5$)



(f) Eqn(13) vs. θ for case e.

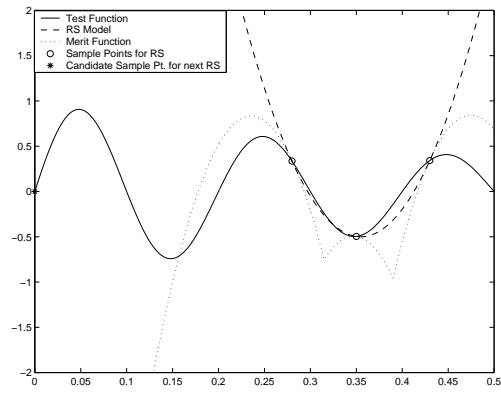


(g) Kriging Model with Gradient Information

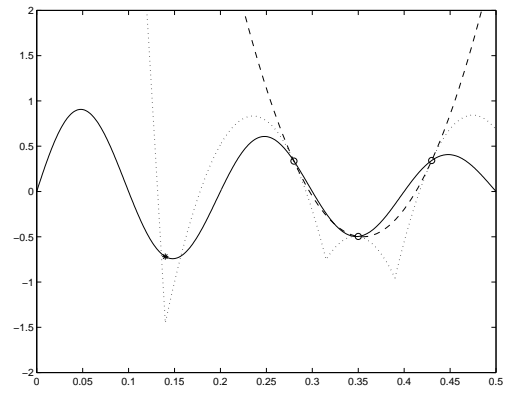


(h) Eqn(13) vs. θ for case g.

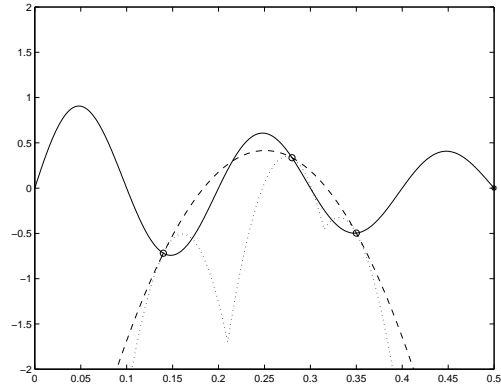
Fig. 5 Test of Correlation Parameter Selection for Kriging



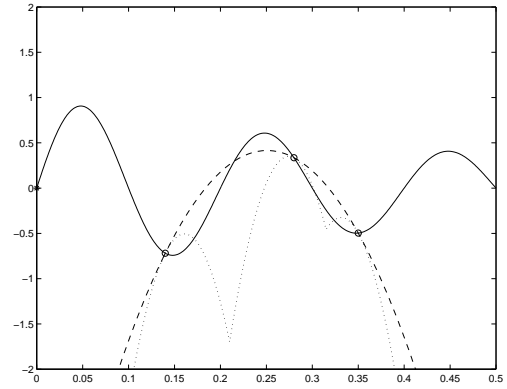
(a) 1st Optimization Cycle



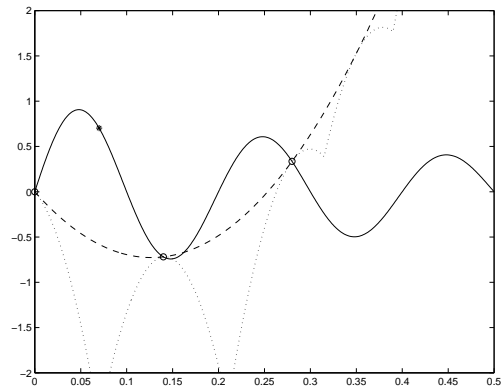
(b) 2nd Optimization Cycle



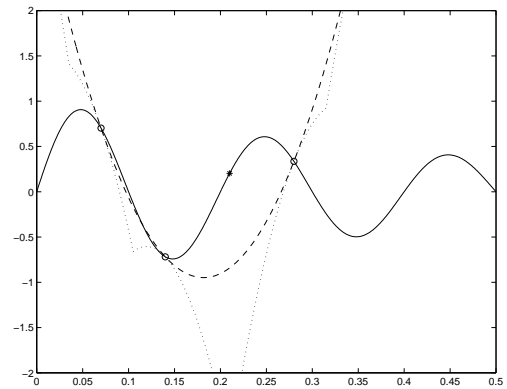
(c) 3rd Optimization Cycle



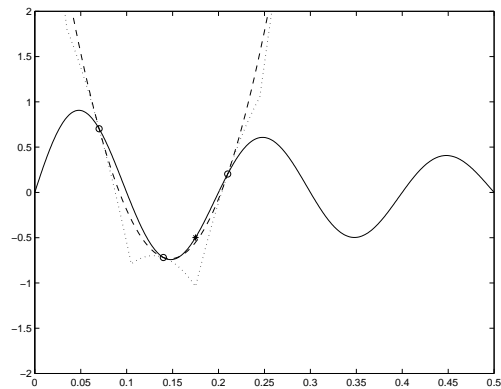
(d) 4th Optimization Cycle



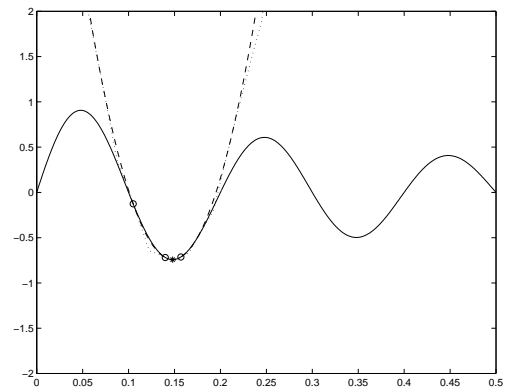
(e) 5th Optimization Cycle



(f) 6th Optimization Cycle

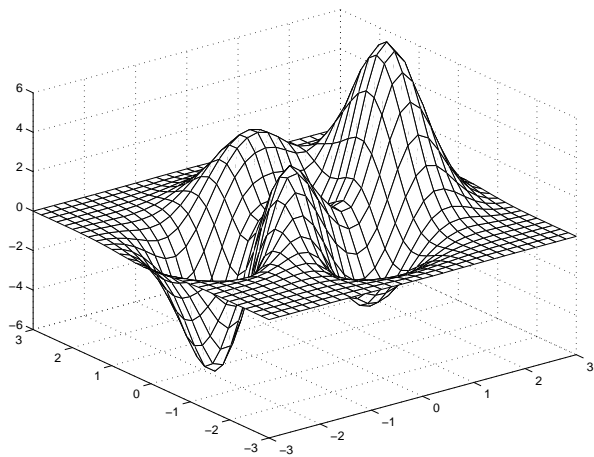


(g) 7th Optimization Cycle

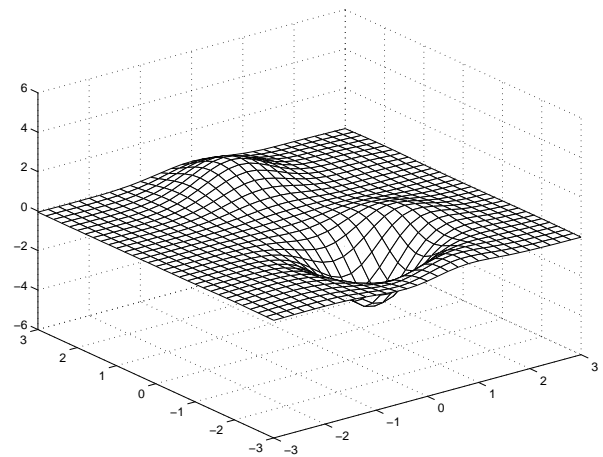


(h) 10th Optimization Cycle

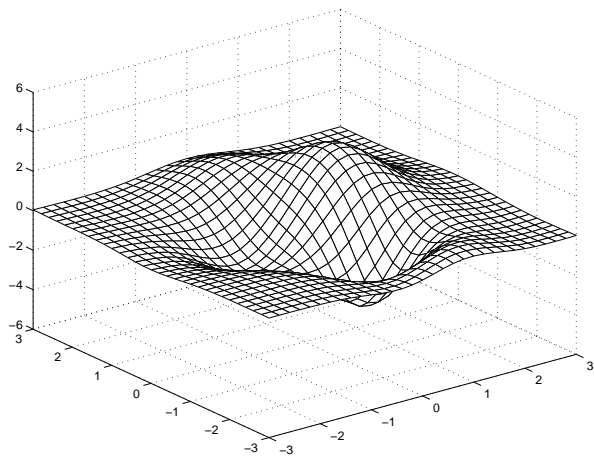
Fig. 6 1-D Optimization with RS+Merit Function: Example of its ability to predict global min.



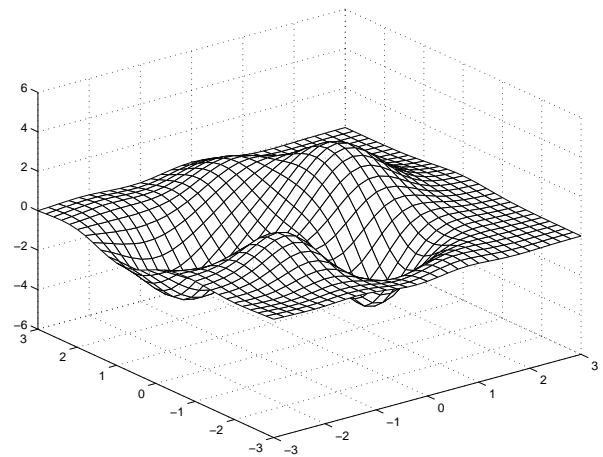
(a) 2-D Analytic Test Function



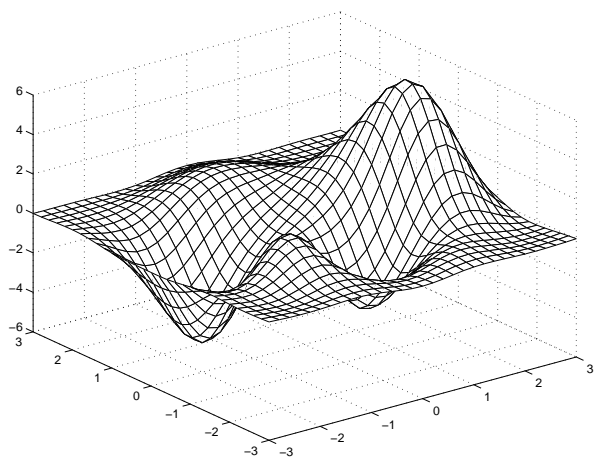
(b) 6th Optimization Cycle



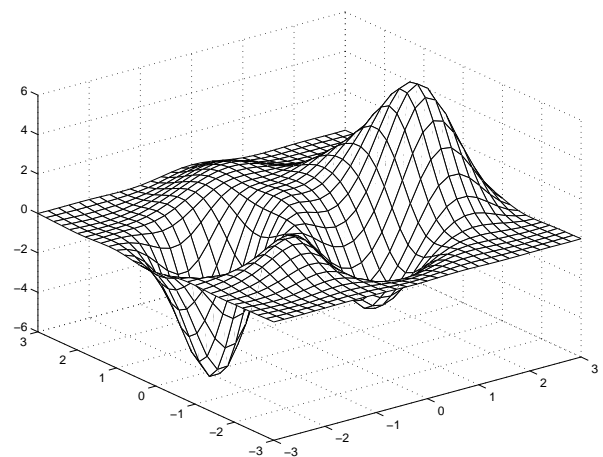
(c) 10th Optimization Cycle



(d) 20th Optimization Cycle

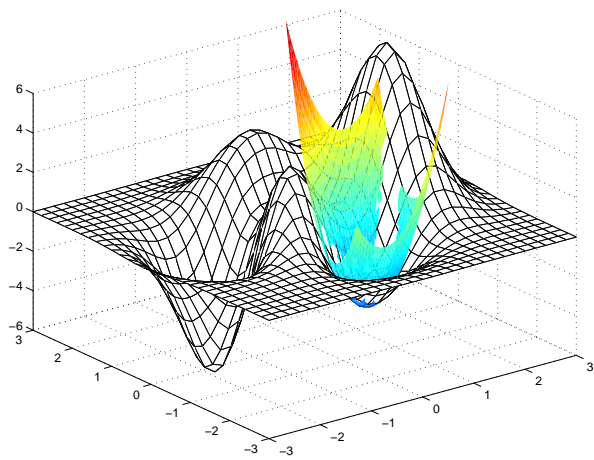


(e) 27th Optimization Cycle

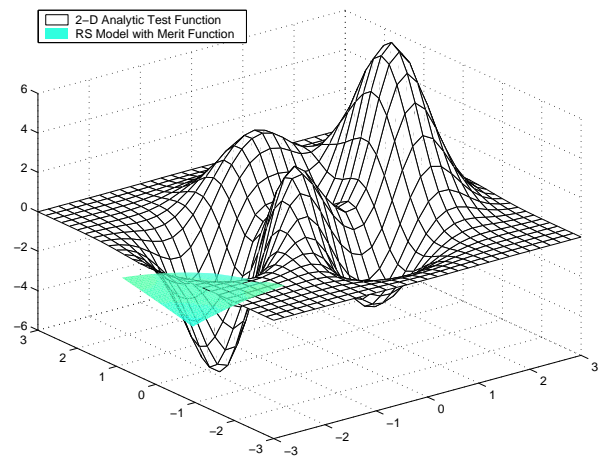


(f) 32nd Optimization Cycle

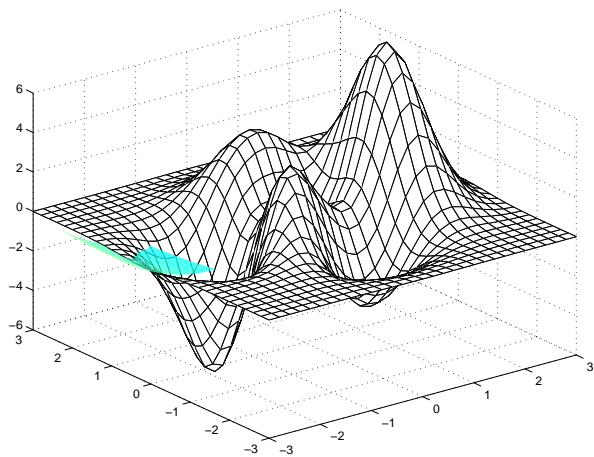
Fig. 7 2-D Optimization with Krig+Merit Function: Example of Kriging's improved ability to predict global minimum (The number of initial sample points are 7.)



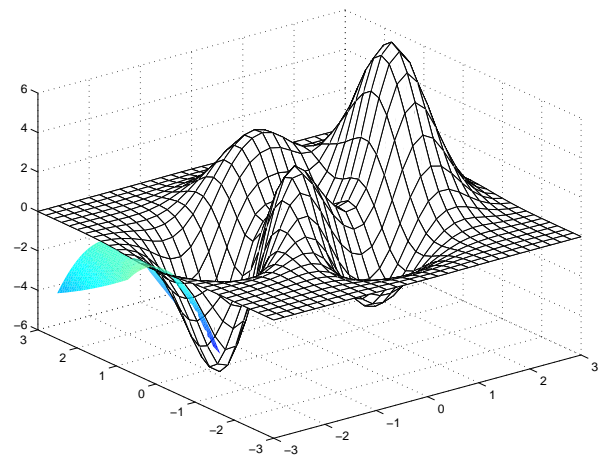
(a) 1st Optimization Cycle



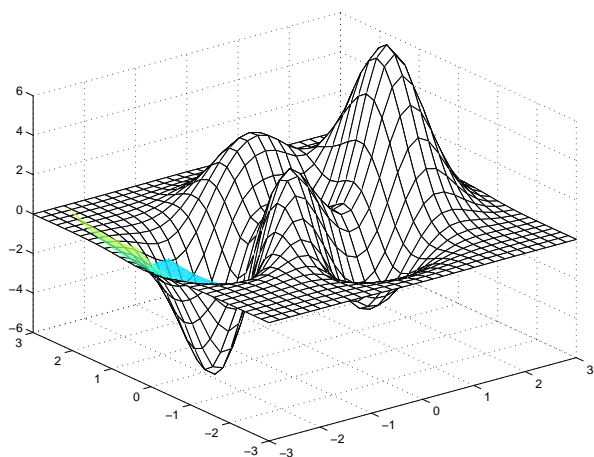
(b) 4th Optimization Cycle



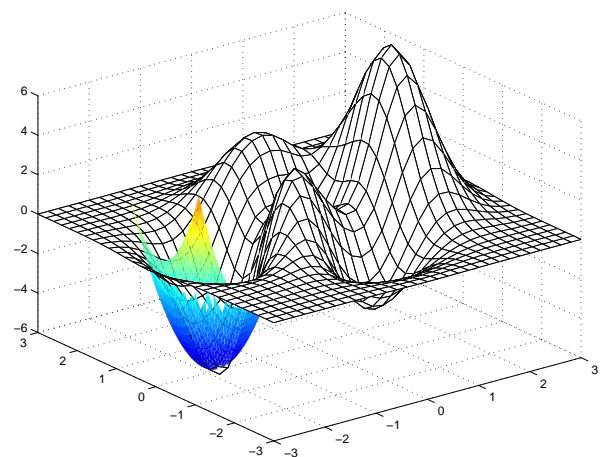
(c) 5th Optimization Cycle



(d) 6th Optimization Cycle



(e) 7th Optimization Cycle



(f) 9th Optimization Cycle

Fig. 8 2-D Optimization with RS+Merit Function: Example of ability of RS+Merit function to predict global minimum.